The influence of doping with Ca and Mg in YBa$_2$Cu$_3$O$_{7-\delta}$ ceramic

S. Attaf[a 1], M. F. Mosbah[1], A. Vecchione[2] and R. Fittipaldi[2]

[1] Université Mentouri. Laboratoire Couches Minces et Interfaces. Campus de Chaabet Erssas - 25017 Constantine, Algéria.
[2] CNR-SPIN and Dipartimento di Fisica "E. R. Caianiello" Università di Salerno, I-84084 Fisciano (SA), Italy

Abstract. We have investigated the effect of partial substitution of Ca for Y and/or Mg for Cu on structural, compositional and magnetic properties in YBa$_2$Cu$_3$O$_{7-\delta}$ polycrystalline compounds. All prepared samples were found to be single phase with small fraction of Ba-secondary phases. Substitution by more than 2% of magnesium causes an increase of spurious phases. Energy Dispersive Spectroscopy (EDS) revealed that the distribution of Ca in the sample is quite homogenous. DC susceptibility measurements show that superconducting transition temperature Tc is reduced much more by Ca than Mg. Hysteresis loops reveal that magnetic irreversibility is decreased by Ca and Mg content. The deduced critical current density Jc does not follow the same variation. Ca alone reduces Jc for x=0.1 and x=0.2. Together with Ca, Mg compensates the reduction of Jc and increasing its content near the solubility limit gives higher Jc than in the undoped sample.

1 Introduction

The analysis of impurity effects in high temperature superconductors (HTSC) gained additional interest upon confirmation that this subject could provide a crucial test for d-wave symmetry of the order parameter in high *Tc* copper oxides [1,2]. Nonisovalent substitutions in YBa$_2$Cu$_3$O$_{7-\delta}$ (YBCO) influence the redistribution of the oxygen atoms in the lattice which is, on the whole, the combination of two effects: influence of the impurity itself and the oxygen content change. It is well known that the oxygen content affects the crystal structure, electronic transport and superconducting properties in YBCO. It is also realized that the superconducting transition temperature, Tc, sensitively depends on both the hole concentration in the CuO$_2$ planes and the relative electric charge of the oxygen within the planes [3,4]. The level of this charge can be controlled either by manipulating the oxygen stoichiometry in the Cu–O chains, by application of pressure or by ionic substitution [5,6].

In pure YBCO, Ca doping is able to revive the superconductivity of deoxygenated material while thestructure remains tetragonal [7]. However, in the fully-oxygenated YBa$_2$Cu$_3$O$_y$; (y =6.93), Ca doping will decrease Tc [1,8]. The reason is that Ca doping is accompanied by a reduction in oxygen content. XRD analysis reveals that such substitution does not lead to changes in the structural

---

[a] e-mail : attaf.sonia@yahoo.fr

symmetry of YBCO [1,2], but a decrease in the orthorhombicity of the system with increasing doping level of Ca is observed [8]. The study of non-magnetic cation substitution in HTSC has generated a thoroughly interest in the last years due to the observation of a very high efficiency in depressing Tc in these materials. This is now known to be an indication primarily of the d-wave symmetry of the superconducting order parameter [9,10]. The most interesting substitution effects are those where the impurities occupy the CuO_2 planes. In that case the spinless impurities such as Zn^{2+} create a strong elastic scattering simultaneously to the formation of a localized magnetic moment. This is indeed the origin of the strong coupling between charge and spin dynamics in these systems [11].

We report here a study of the effect of partial substitution of Ca for Y, of Mg for Cu and the double substitution of Ca in Y site and Mg in the place of Cu on structural and magnetic properties of $YBa_2Cu_3O_{7-\delta}$ compounds.

2 Experimental details

All YBCO samples were synthesized by standard solid state reaction of stoichiometric mixture of Y_2O_3, $CaCO_3$, $BaCO_3$, MgO and CuO at 750 °C and 900 °C for 5 h. This was followed by annealing in air at 915°C, 930°C, 940°C for 24 h. The samples were then heated at 940 °C in flowing O_2 at 1.5 bar for 6 h followed by rapid cooling to 400°C, then 400 °C for 24h and finally furnace cooled down to room temperature. In order to achieve the best results the powders were ground thoroughly (45 minute for 5g of powder) before the first firing and the intermediate grindings, made before each annealing, were fast (about 15 minute) to avoid possible effects of atmospheric moisture on the samples.

The structure and phase purity of samples were examined by the X-ray powder diffraction technique (XRD) performed by means of a D8 Advance Bruker diffractometer with $Cu_{K\alpha}$ radiation. The grain morphology of surface of the samples was analyzed by scanning electron microscopy (SEM). Compositional analysis of grains was determined by Energy Dispersive Spectrometry analysis (EDS) using an INCA Oxford analyzer. The magnetic properties were obtained from Zero Field Cooled (ZFC) and Field Cooled (FC) M(T) DC magnetization measurements, and M(H), using a Physical Properties of Materials System (PPMS) of Quantum Design working in a vibrating samples magnetometer (V.S.M.) mode.

3 Results and discussion

3.1 Phases identification

XRD patterns (Fig. 1) of polycrystalline materials of composition $YBa_2(Cu_{1-y} Mg_y)_3O_7$ with y ≤ 0.15 revealed that all prepared samples are orthorhombic. The diffraction lines corresponding to spurious phases appear for $x \geq 0.02$ they can be easily identified and are indicated in Fig.1. Their fraction increases much more with Mg content. We note that the angular position of the peaks for low doping level x <0.04 changes significantly with the introduction of magnesium. For high doping level the main lines are shifted to higher angle side as Mg content increases suggesting that *c* axis decreases and some dopant ions occupy the lattices sites. The analysis of XRD patterns related to selected $Y_{1-x}Ca_xBa_2Cu_3O_{7-\delta}$ sample were indexed also in the orthorhombic phase, even at the highest value of x. Their patterns are like that of $Y_{1-x}Ca_xBa_2(Cu_{1-y}Mg_y)_3O_{7-\delta}$ system because of very low concentration of Mg doping in Cu sites (Fig. 2). The samples with concentration x=5% and 10% of Ca shows the presence of a certain degree of orientation in pellets. The important change in intensity ratios between (00*l*) reflections and other reflections indicates significant regions of samples oriented. All prepared samples show a small fraction of Ba-secondary phases at values of 2θ between 28° and 31° indicating a partial substitution of Ca at the Ba sites. The main impurity was identified as $BaCuO_2$, the creation of Cu vacancies is then also possible [12]. The doubling and

splitting of the main reflection (013) and (103) is less significant as Mg and Ca contents increase, the doping promotes then the orthorhombic to tetragonal transition.
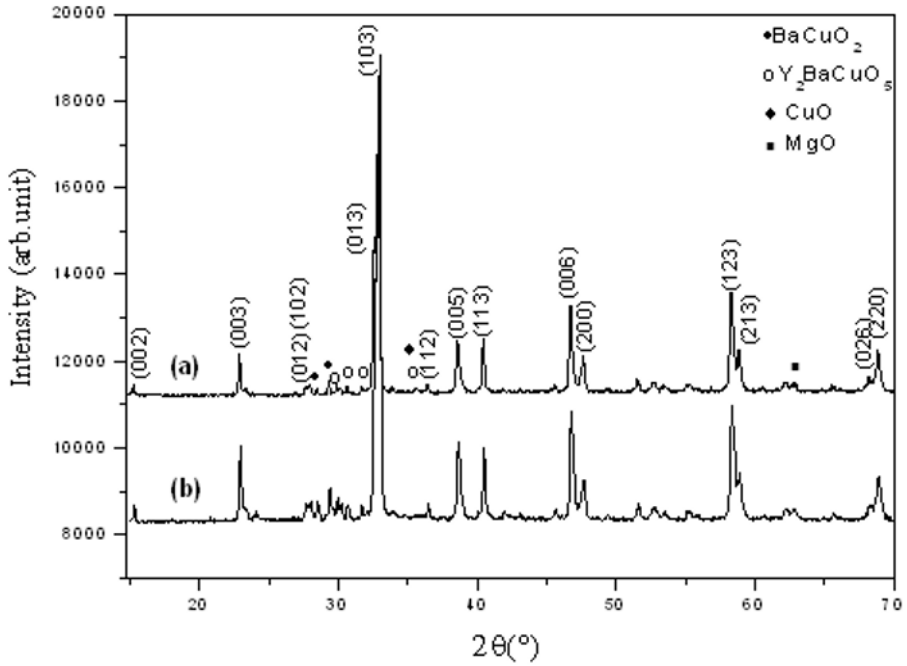

Fig.1. XRD patterns of YBa$_2$(Cu$_{1-y}$Mg$_y$)$_3$O$_{7-\delta}$ samples with: (a) y= 0,05 (b) y=0.1

Fig.2. XRD patterns for Y$_{1-x}$Ca$_x$Ba$_2$ (Cu$_{1-y}$Mg$_y$)$_3$O$_{7-\delta}$ for y =0.02 : (a) pure system, (b) x= 0.05, (c) x= 0.1, (d) x= 0.15 and (e) x=0.2

3.2 SEM measurements

Fig.3 shows SEM photographs of the samples doped with Mg, taken at the same magnification, which reveal homogeneous grains. The grains become much finer, almost with spherical shape and bad connected as Mg contents increases. The difference is clear for samples doped with high Ca contents and low Mg contents (Fig. 4.b), where we can see formation of stick shape grains with random orientation and best connectivity between the grains.

One can see also from Fig.4 that as the concentration of Ca increases the average grain size decreases. The co doping with Ca and Mg has induced finer, best connected and closely packed grains which can improve the percolation path of the current and so it is easier for the current to avoid the worse grains. The finer grain would bring more disorder in the grain boundary region, which results in vortex pinning centres increasing and subsequently enhances the critical current density [13].
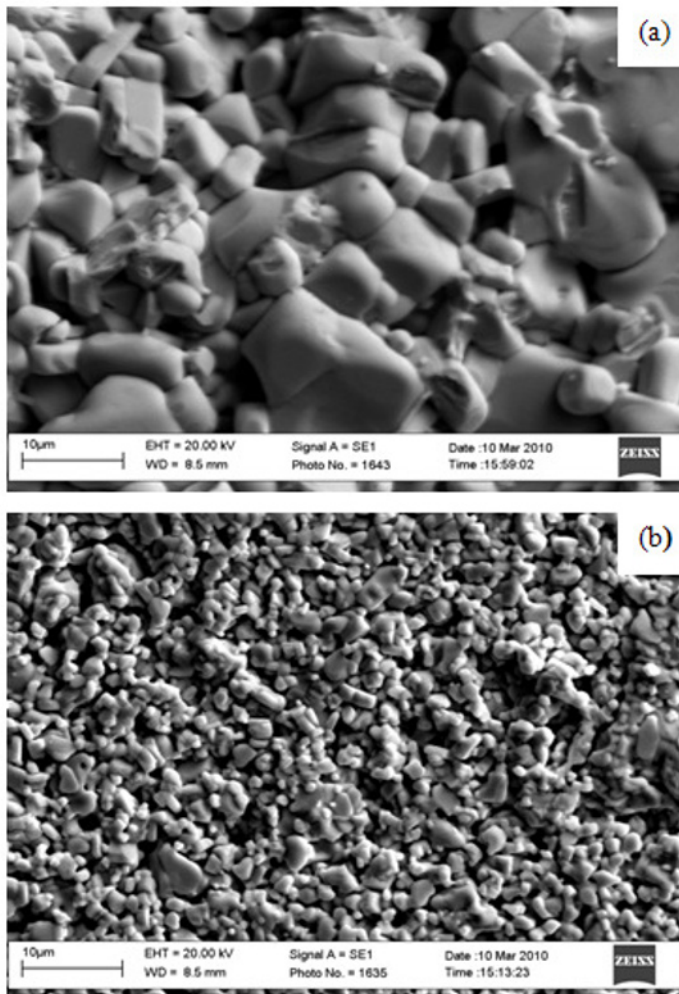

Fig.3. The SEM photographs of samples doped with: (a) 1 %Mg, (b) 4% Mg

The incorporation of the Ca and Mg into the grains as the local stoichiometry was confirmed by means of EDS on various region and area of the same samples and are consistent with our XRD analysis. Table 1 and 2 summarise the grains analysis of co doped YBCO samples. It was revealed

contrary as reported in [13](for Ca) that the distribution of the Ca in the sample is quite homogenous while the distribution of the MgO particles seems to be inhomogeneous.

Table 1. Grains analysis of $Y_{1-x}Ca_xBa_2(Cu_{1-y}Mg_y)_3O_{7-\delta}$ samples for y = 0.01. Significant amount of Mg is detected only for sample with 20% of Ca and for 20 grains examined two grains contain high concentration of magnesium. No grains with spurious phases were detected

Nominal value of x	Number of EDS examined grains	Number of homogeneous Y-123 grains	Number of -substituted grains		Effective value of x determined by EDS	Composition determined by EDS
			Ca	Mg		
0.00	15	15	0	0	0.00	$Y_{1.11}Ba_2Cu_{2.85}O_{9.51}$
0.05	15	3	9	0	0.05	$(YCa)_{1.01}Ba_2Cu_{2.90}O_{8.24}$
0.10	15	0	15	0	0.09	$(YCa)_{1.04}Ba_2Cu_{2.81}O_{8.66}$
0.15	21	1	20	0	0.15	$(YCa)_{1.00}Ba_2Cu_{3.35}O_{9.95}$
0.20	21	0	19	2	0.20	$(YCa)_{0.94}Ba_2(CuMg)_{2.86}O_{10.18}$

Table 2. Grains analysis of $Y_{1-x}Ca_xBa_2(Cu_{1-y}Mg_y)_3O_{7-\delta}$ samples for y = 0.02

Nominal value of x	Number of EDS examined grains	Number of homogeneous Y-123 grains	Number of -substituted grains		value of x determined by EDS	Composition determined by EDS	Number of spurious phases grains	
			Ca	Mg			Y_2BaCuO_5	$BaCuO_2$
0.05	20	2	17	3	0.05	$(YCa)_{0.87}Ba_2(CuMg)_{2.96}O_{6.84}$	0	0
0.10	20	0	18	2	0.11	$(YCa)_{0.88}Ba_2(CuMg)_{3.00}O_{7.25}$	0	0
0.15	20	0	18	1	0.16	$(YCa)_{0.77}Ba_2(CuMg)_{2.87}O_{7.87}$	0	1
0.20	20	0	19	1	0.20	$(YCa)_{0.90}Ba_2(CuMg)_{3.12}O_{7.84}$	0	0

3.3 Magnetization measurements

FC and ZFC magnetization versus temperature measured under a DC magnetic field of 10 Oe (50 Oe for the samples doped with Mg only) are shown in figures 5 and 6. The undoped sample exhibits a Tc~ 91.85 K which shows that the doping and the oxygen content are near the optimum. The XRD results of this sample have revealed the YBCO-phase as a major phase. The ZFC M(T) curve of this sample shows when the applied field is 10 Oe a feature at about 70 K which is not seen when the applied field is 50 Oe. This effect is thus a result of the opening of the weak links and not of the occurrence of secondary phases in the sample. The samples doped only with Mg exhibit an important decrease in their Tc$_{onset}$ (defined as the temperature of the onset of diamagnetism). This decrease is about 15 to 20 K and the width of the transition increases. For samples doped only with Ca content, the decrease in Tc is less important (about 10 K). This is due to the fact that the Ca doping in YBCO shrinks the misaligned region at the Grains boundary cause of most electrical resistance, both in width and height [14] but the change between a content of Ca x = 0.1 and x = 0.2 is not important while the width of the transition is increased by about 50 %. The depression of Tc is an indication that Ca and Mg have moderate effect on the conduction mechanism and magnetic order. When the samples are co doped with Ca and Mg, both ZFC and FC curves show a decrease of the width of the transition when the content of Mg is increased. The change of charge carrier density due to doping with Mg [15-16], the induction of mobile holes by substitution with Ca [17-18] coupled or no with various structural changes [19], overall oxygen content and the disorder in Cu-O$_2$ planes [8-20] are various mechanisms responsible for variation of Tc. The magnetization curves show also that the

amount of the difference ΔM between the Meissner effect (FC) response and the effect of the shielding current lines (ZFC) increases with Ca content and decreases with Mg content. ΔM represents the trapped flux in the sample and is influenced for very low applied field by the intergrain and the intragrains current. In other words, both the grains size and the quality of the grains boundary have an effect on ΔM. The SEM observations show that both Ca and Mg reduce the average grain size. Thus, the increase of ΔM in the Ca doped samples cannot be the effect of the grain size but is an indication of the enhancement of the grains boundary quality.
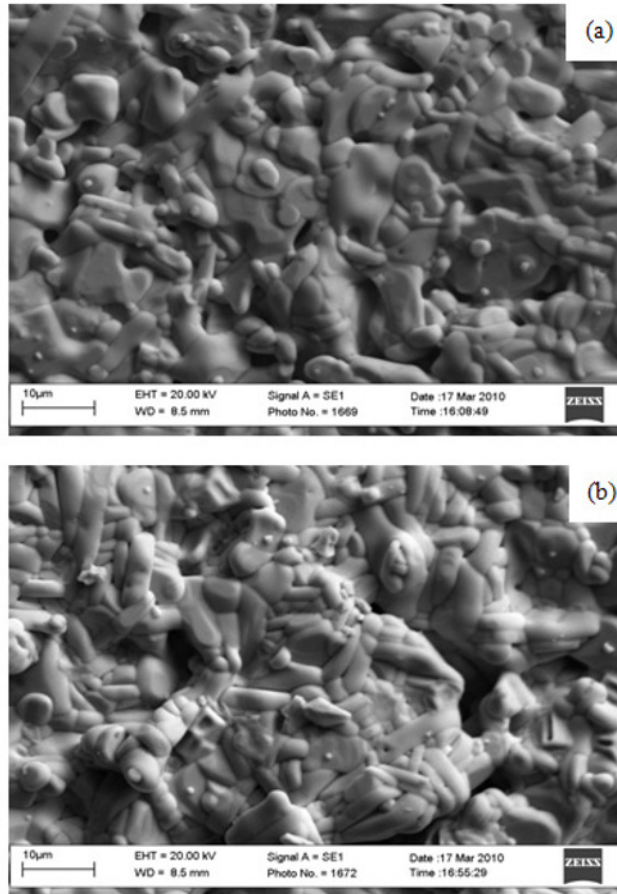

Fig.4. The SEM photographs of samples with 2% Mg and (a) 5 %Ca, (b) 15% Ca

The hysteresis loops of samples at 4.2 K (Fig. 7) at high magnetic field (Parallel field arrangement) present the same shape and indicate that the magnetisation M decreases as the concentration of Mg and Ca increases. The sample showing the best texture, deduced from XRD analysis, has the highest M as reported in [21]. For the other samples the decrease in grain size, induced by doping, corresponds to a reduction in M. In first sight, the reduction of grain size reduces the current loops and consequently the magnetisation M. One sample, doped with 5% Ca and 1% Mg does not obey this scheme.

The critical current density has been deduced from the curves of Fig. 7 by use of Bean's model. Taking into account the average grain size, the used formula is $Jc = 30M_{irr}/R$ where M_{irr} represents the difference between the upper and the lower parts of the cycle taken for the positive values of H [22] and R the average radius of the grains. The calculated Jc is shown in Fig. 8. Considering fields above 20 kOe, where the demagnetising field and other shape and surface effects may be ignored, Jc

follows the same variation of M with the concentration of Ca except for a content of 2% of Mg where the doped samples exhibit a higher Jc than the pure sample one and a variation versus the content of Ca going through a minimum. When 1% Mg is introduced the Jc is enhanced without exceeding the pure sample one (except for 5% Ca content). On the other hand, Jc is nearly constant for an applied field 40 kOe and 80 kOe when the sample is doped with 20% Ca and 1% Mg. Without Mg, the samples doped with Ca exhibit a Jc lower than the undoped sample one. This behaviour has been observed, in thin films, only when the content of Ca is about 20% [23]. The enhancement of Jc has been observed, at 60K and 70K, when the grain boundary, not the grain itself, is doped with Ca [24]. The reduced Jc may be due to chain disorder induced by Ca doping. The co doping with Mg seems to compensate the effect of Ca on the chain disorder. This compensation is also observed in the effects on the width of the transition showed by ZFC and FC M(T) measurements. Mg induces a reduction of the grain size . But Mg, substituting Cu, may also occupy a site on the chains changing the valence from +1 to +2. This variation of charge may explain the enhancement of Jc. The scenario could be that part of Mg atoms substitute on Cu_2O plan sites, reducing Tc, and the other part substitute on the chains, enhancing Jc and reducing the width of the transition. The situation of co doping is more complicated than doping with one element. Doping alone, Mg substitutes Cu on Cu_2O planes' site and Jc decreases as reported by various authors [15-25]. Our results show a different behaviour: possibility of substitution on chain's site and enhancement of Jc. More investigation is needed to elucidate, when there is co doping, on what site of Cu Mg substitutes.
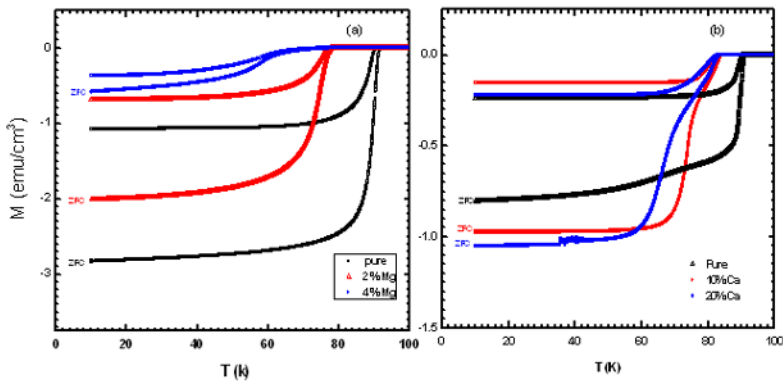

Fig. 5. ZFC and FC *M(T)* curves of : (a) $YBa_2(Cu_{1-y}Mg_y)_3O_7$ samples with an applied DC field of 50 Oe and (b) $Y_{1-x}Ca_xBa_2Cu_3O_{7-\delta}$ samples with an applied DC field of 10 Oe
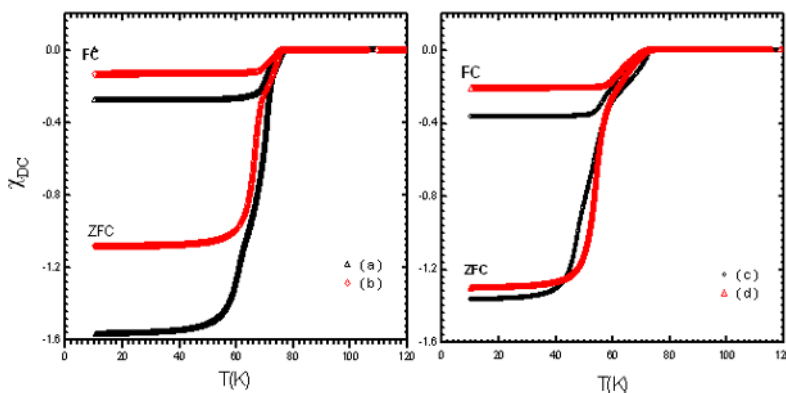

Fig. 6. DC susceptibility of $Y_{1-x}Ca_xBa_2(Cu_{1-y}Mg_y)_3O_{7-\delta}$ samples with an applied field of 10 Oe (a) 1% Mg and 5 %Ca [Tc_{onset}= 76.60k], (b) 2% Mg and 5% Ca [Tc_{onset}= 75.92k], (c) 1% Mg and 15% Ca [Tc_{onset}= 73.50k], (d) 2% Mg and 15% Ca [Tc_{onset}= 72.60k]
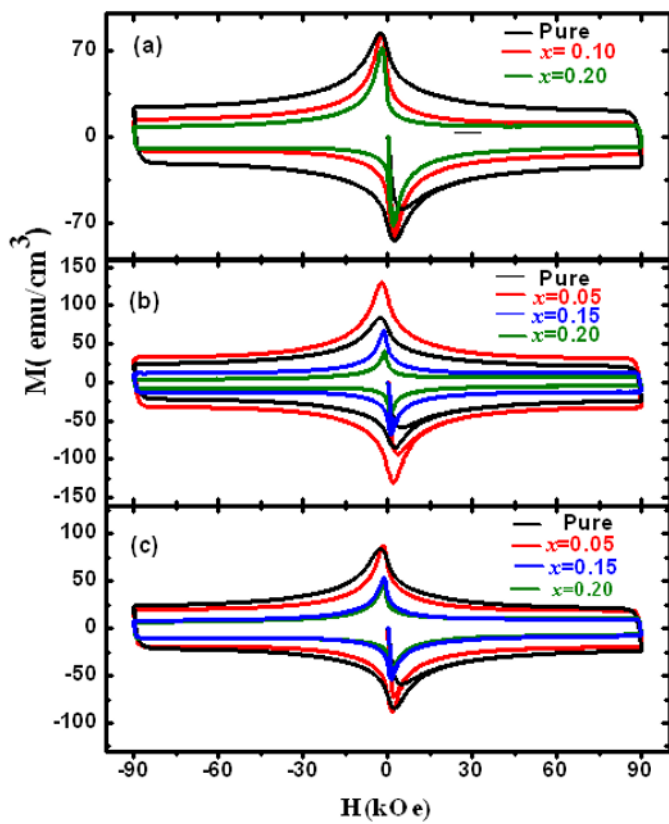
Fig.7. Magnetic hysteresis loops at 4.2K of $Y_{1-x}Ca_xBa_2(Cu_{1-y}Mg_y)_3O_{7-\delta}$ samples with (a) $y=0$, (b) $y=0.01$, (c) $y=0.02$
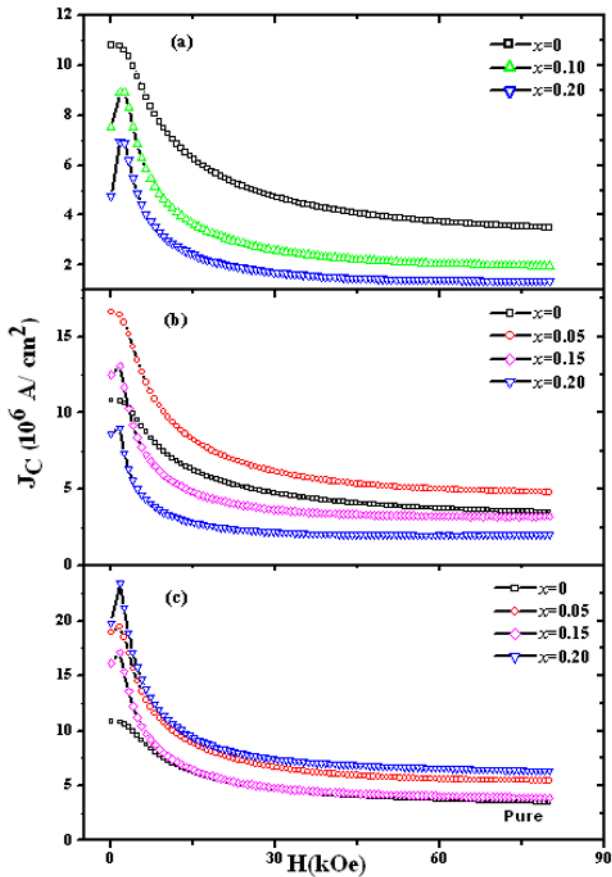
Fig. 8. Critical current densities deduced using Bean's model from M(H) curves of Fig. 7 for samples with (a) $y=0$, (b) $y=0.01$, (c) $y=0.02$

4 Conclusion

The effects of partial substitution of Y by Ca, Cu by Mg and the double substitution of the same elements have been studied in polycrystalline $YBa_2Cu_3O_{7-\delta}$. EDS analysis shows an homogenous distribution of Ca in the sample. Mg reduces Tc much more than Ca but substituted together with Ca reduces the width of the transition. Substitution by Ca alone reduces Jc for $x=0.1$ and $x=0.2$. Substituting by Mg together with Ca seems to have a compensating effect which enhance Jc and leads to values higher than those of the pure sample when the content of Mg is near the solubility limit.

References

1   X. S. Wu, S. S. Jiang, J. Lin, J. S. Liu, W. M. Chen, X. Jin, Physica C **309** 25 1998.
2   R. Giri, V. P. S. Awana, H. K. Singh, R. S. Tiwari, O. N. Srivastava, Anurag Gupta, B. V. Kumaraswamy, H. Kishan, Physica C **419** 101 2005.
3   M. Karppinen, H. Yamauchi, J. Inorg. Mater. **2** 589 2000.
4   J. J. Capponi, C. Chaillont, A. W. Hewat, P. Lejay, M. Mariezio, N. Nguyou, B. Raveau, J. L. Sonbeyroux, J. Tho-lence, R. Tounier, Eur. Phys. Lett. **3** 1301 1987.
5   H. Yamauchi, M. Karppinen, Supercond. Sci. Technol. **13** R33 2000.

6   R. Beyers, T. M. Shaw, Solid State Phys. **42** 135 1989.
7   P. Starowicz, J. Sokolowski, M. Balanda, A. Szytula, Physica C **363** 80 2001.
8   V. P. S. Awana, A. V. **Narlikar**, Phys. Rev. B **49** 6353 1994.
9   C. Bernhard et al, phys. Rev. Lett.**77** 2304 1996.
10 A. J. Zaleski. J. Klamut, Phys. Rev. B **59**, 14023 1999.
11 P. Mendels et al, Europhys. Lett.**46** 678 1999.
12 F. Ben Azzouz , M. Zouaoui, K. D. Mani, M. Annabi, G. Van Tendeloo and M. Ben Salem *Physica* C **442** 13 2006.
13 Ke-XiXu, Jing-He Qiu and Li-yi Shi, Supercond. Sci. Technol. **19** 178-183 2006.
14 M.A. Schofield, M. Beleggia, Y. Zhu, K. Guth, C. Jooss, Phys. Rev. Lett **92** 195502 2004.
15 L. Raffo, R. Caciuffo, D. Rinaldi and F. Licci *Supercond. Sci. Technol.* **8** 409 1995.
16 A. Vyas, C. C. Lam and L. J. Shen *Physica* C **935** 341-348 2000.
17 J. L. Tallon, C. Bernhard, H. Shaked, R. L. Hitterman and J. D. Jorgensen *Phys. Rev.* B **51** 12911 1995.
18 Y. Tokura, J. B. Torrance, T. C. Huang and A. L. Nazzal *Phys. Rev.* B **38** 7156 1988.
19 V. P. S. Awana, S. K. Malik, W. B. Yelon, A. Claudio. Cardoso, de Lima O F, A. Gupta, A. Sedky, S. B. Samanta and A. V. Narlikar *Physica* C **338** 197 2000.
20 V. P. S. Awana, S. K. Malik and W. B. Yelon *Physica* C **262** 272 1996.
21 S. J. Senoussi *Phys. III France* **2** 1041 1992.
22   A. G. Loeser, Z. X. Shen, D. S. Dessau, D. S. Marshall, C. H. Park, P. Fournier, A. Kapitulnik, Science **273** 325 1996.
23 S. H. Naquib and A. Semwal, Physica C **425** 14 2005.
24 Y. Zhao and C. H. Cheng, Physica C **386** 286 2003.
25 J. Figueras, A. E. Carrillo, T. Puig and X. Obradors, J. Low Temp. Phys. **117** 873 1999.